EARTHQUAKE ENGINEERING AND STRUCTURAL DYNAMICS, VOL. 26, 501–513 (1997)

INELASTIC SEISMIC RESISTANCE OF REINFORCED CONCRETE STACK-LIKE STRUCTURES

ALOK GOYAL[1†] AND MANOJ K. MAITI[1‡]

[1]*Department of Civil Engineering, Indian Institute of Technology, Powai, Bombay 400076, India*

SUMMARY

A method is presented to quantify the inelastic seismic resistance of reinforced concrete stack-like structures by non-linear earthquake analysis. The deformed configuration of stack is idealized as an assemblage of beam elements and actual stress–strain relationships of concrete and reinforcing steel are used to evaluate element matrices. Repeated non-linear analyses are performed by gradually increasing the intensity of acceleration time histories to a level where collapse of the stack is observed in primary stresses. The set of time histories thus obtained are then used to define the ultimate intensity of ground motion that the stack can sustain if inelastic deformations are permitted. A procedure is presented to quantify the difference between inelastic seismic resistance and elastic seismic resistance in terms of displacement ductility capacity factors. For seismic design using available inelastic resistance, values of curvature ductility factor demand for the cross-sections of stacks are also presented. © 1997 by John Wiley & Sons, Ltd.

KEY WORDS: stacks; chimneys; towers; ductility; seismic design; inelastic response

INTRODUCTION

In the development of seismic design provisions for structures, a widely accepted approach is to provide strength based on elastic analysis for a design-level earthquake, and keep provisions for significant inelastic deformations (and limited damage) for intense ground motion that may occur rarely during the life of structure. However, codes are not explicit about the interaction between elastic design strength and actual seismic resistance in the inelastic range, usually measured by ductility capacity. For building structures, ductility has been well investigated and design details incorporated in codes. However, lack of research on ductile behaviour of reinforced concrete stack-like structures, such as towers and chimneys, and on the collapse threshold for such structures subjected to strong ground motions, precludes reliable evaluation of their actual seismic resistance. For many years, it has been assumed that in stack-like structures, it would be difficult to develop lateral displacement ductility factor in excess of two[1,2] because extensive yielding of one section may lead to extensive displacements and eventually collapse. Therefore, most of the design standards, for example, ACI-307-79,[3] specify increased design earthquake force-level for stack-like structures than those for buildings, basically not to impose large ductility requirements on such structures. Even then, the design forces in stack-like structures correspond to a displacement ductility factor of 2–5.[1]

The redistribution of forces is not possible in statically determinate stack-like structures, and yielding of a single section may be sufficient to cause failure under sustained loads. However, earthquake forces act for a very short duration and rapidly change direction several times and, therefore, dynamic stability of a stack in the inelastic range cannot be ruled out. From design considerations, stacks can be permitted to undergo

† Associate Professor
‡ Formerly Graduate Student

CCC 0098–8847/97/050501–13$17·50

Received 19 August 1994
Revised 29 August 1996

inelastic deformations during seismic event because experimental tests have demonstrated that properly detailed, hollow circular cross-sections are capable of mobilizing sufficient curvature ductility.[4] To use this aspect in seismic design, the actual seismic resistance of stacks need be quantified so that provisions are made for inelastic deformations in stacks during intense ground motion.

A procedure is presented in this paper for quantifying the inelastic seismic resistance of reinforced concrete stack-like structures by non-linear earthquake analysis. A method is also proposed to estimate the overall displacement ductility capacity factors for stacks. Attempts have been made to estimate the curvature ductility factor demand for the cross-sections of stack so that the available inelastic resistance could be effectively utilized in seismic design.

NON-LINEAR EARTHQUAKE ANALYSIS

Idealization of stack

The system considered consists of a tapered reinforced concrete stack with hollow circular cross-section fixed at the base. The stack cross-sections are provided with two rings of longitudinal reinforcements and cages of circumferential reinforcement placed near both the inside and outside faces of the section (Figure 1). It is assumed that the bar sizes and spacing of circumferential steel, selected in detailing, are appropriate to prevent premature buckling of the longitudinal reinforcement, and to provide sufficient shear resistance so that the collapse of the stack is due to crushing of concrete in primary stress arising from axial load and flexure. The stack is analysed for a single horizontal component of free-field ground acceleration, and therefore, only planar vibrations of stack are considered in this investigation.

An incremental step-by-step finite element procedure is followed for the non-linear analysis, in which solution is obtained at closely spaced discrete time steps. The deformed configuration of stack is idealized as an assemblage of sufficiently large number of straight two-noded beam elements that include only axial and bending deformations. For each beam element, a local co-ordinate system x–y passing through two end nodes, is defined (Figure 2). The origin and direction of this co-ordinate system are continuously updated according to current positions of the two end nodes. Thus, rigid-body motions are eliminated and the assumption of small displacement theory remains valid when the incremental displacements of element for next load step are referred to this local co-ordinate system. Equilibrium equations for each element are

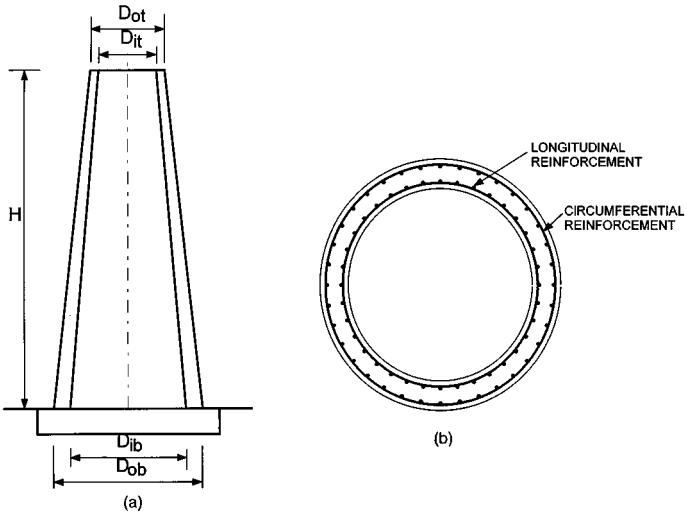

Figure 1. Typical reinforced concrete stack-like structure: (a) stack; (b) cross-section

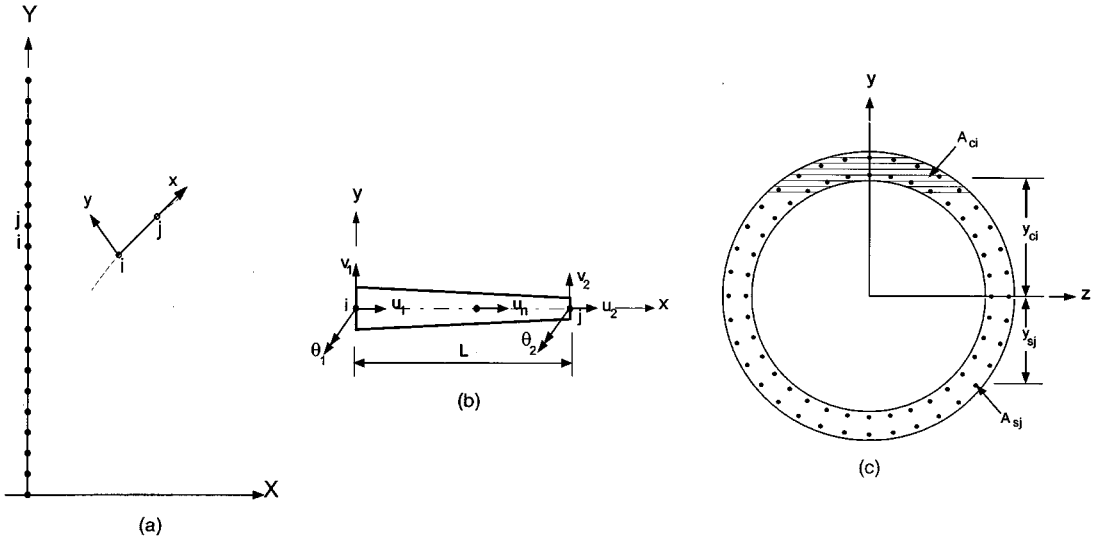

Figure 2. Finite element model of stack-like structure: (a) idealized stack; (b) beam element; (c) idealization of cross-section

written in local co-ordinate system and then transformed to the fixed global X–Y co-ordinate system by using transformation matrices that are continuously updated.

The centroidal axis of beam element has been selected as reference axis in the finite element formulation. Axial displacement at centroidal axis is computed from nodal displacements at beam ends, u_1 and u_2, using linear interpolation functions (Figure 2). Because of cracking and material non-linearity, neutral axis may not coincide with the reference axis, and therefore, an additional incompatible axial degree of freedom, u_n, at mid-point of the element is considered to allow linear variation of axial strain along the reference axis.[5] This incompatible degree of freedom is, however, condensed out at the element level. The transverse displacement of reference axis is computed from nodal displacements in transverse direction, v_1 and v_2, and rotations θ_1 and θ_2 at beam ends, using standard cubic Hermitian interpolation functions.[6] The axial displacement $u(x, y)$ and transverse displacement $v(x, y)$ at any point within beam element are obtained by the Euler–Bernoulli beam kinematics, i.e.

$$u = u_0 - y\frac{\mathrm{d}v_0}{\mathrm{d}x}, \qquad v = v_0 \tag{1}$$

where $u_0(x)$, $v_0(x)$ are the displacements of centroidal axis along the x- and y-axis, respectively. The axial strain, $\varepsilon(x, y)$, at any point is then expressed as

$$\varepsilon = \left[\frac{\mathrm{d}u_0}{\mathrm{d}x} - y\frac{\mathrm{d}^2v_0}{\mathrm{d}x^2}\right] + \left[\frac{1}{2}\left(\frac{\mathrm{d}v_0}{\mathrm{d}x}\right)^2\right] \tag{2}$$

At each Guass point, the stack cross-section is discretized into a number of strips parallel to the neutral axis (Figure 2). For each strip of concrete, stress at any instant of time is computed according to the strain at centroid of the strip using cyclic stress–strain relationship of concrete. Similarly, each reinforcing bar is idealized independently and the stress in each reinforcing bar is computed according to the strain at its centroid using the cyclic stress–strain curve for reinforcing steel. The stress–strain relations of concrete and reinforcing steel used in this study are presented next.

Stress–strain relationships for concrete and reinforcing steel

The mathematical model for cyclic stress–strain relationship of concrete is shown in Figure 3. The envelope of cyclic stress–strain curves in compression is represented by the curve obtained by monotonically increasing the load. The envelope curve consists of a second degree parabola for the ascending branch and a linear softening branch.[7] The parabolic part is represented by

$$\sigma_c = \sigma_{cy}\left[\frac{2\varepsilon_c}{\varepsilon_{cy}} - \left(\frac{\varepsilon_c}{\varepsilon_{cy}}\right)^2\right] \tag{3}$$

where σ_c and ε_c are concrete stress and strain, respectively, σ_{cy} is the compressive strength of concrete, and $\varepsilon_{cy} = 0{\cdot}002$ is the strain at maximum stress. The linear softening branch is defined by an ultimate compressive strain ε_{cu} and a corresponding stress of $0{\cdot}2\sigma_{cy}$. Concrete is assumed to have no tensile strength.

The cyclic unloading–reloading relation is assumed to be linear. If the maximum imposed strain in concrete is less than ε_{cy}, the slope of the unloading–reloading path is equal to the initial tangent modulus of elasticity E_c. If the maximum imposed compressive strain in concrete is greater than ε_{cy}, the slope of the unloading–reloading path is equal to E_cF_c, where F_c is given by[7]

$$F_c = 0{\cdot}8 - \frac{0{\cdot}7(\varepsilon_{cm} - \varepsilon_{cy})}{\varepsilon_{cu} - \varepsilon_{cy}} \tag{4}$$

in which ε_{cm} is the maximum compressive strain attained. The reduction factor F_c takes into account the degradation of stiffness for both unloading and reloading curves for increasing values of maximum strain.

The stress–strain relationship of reinforcing steel is assumed as a bilinear stress–strain envelope and linear unloading–reloading behaviour upon stress reversal (Figure 3). Stress–strain behaviour of reinforcing steel is taken same in both tension and compression. The slope of the unloading–reloading branch is same as the initial elastic modulus of steel. The reinforcing steel is assumed to fail when the strain in any direction exceeds the ultimate strain ε_{su}. The complete stress–strain behaviour is defined by four parameters: initial modulus of elasticity E_s, strain hardening modulus E_{sh}, yield stress σ_{sy} and ultimate strain ε_{su}.

Equations of motion

The incremental equilibrium equations of motion for stack have been derived from the principle of virtual work. The element matrices in these equations are evaluated by numerical integration over length of the element using Gauss quadrature, and by layer integration over the cross-section at each Gauss point. Before the element matrices are assembled, they are transformed to fixed global co-ordinate system using the updated transformation matrices. The assembled, linearized, incremental equations of equilibrium, including

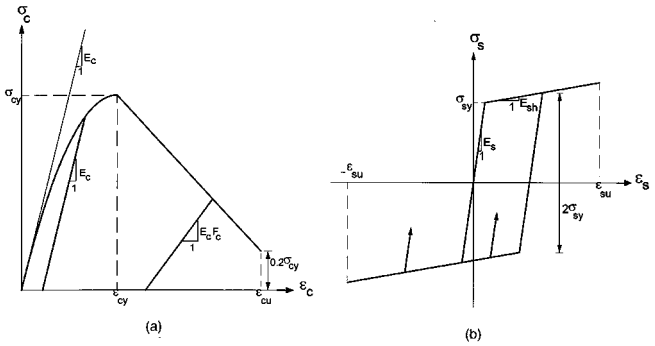

Figure 3. Stress–strain relationships for: (a) concrete and; (b) reinforcing steel

the damping term, for planar vibrations of stack subjected to ground motion $\ddot{u}_g$ at time $t + \Delta t$, where Δt is the increment in time, can be written in the following form[8]

$$(\mathbf{K}_e)_t \Delta \mathbf{v}_t + (\mathbf{K}_g)_t \Delta \mathbf{v}_t = -\mathbf{M}_t(\mathbf{1}_x [\ddot{v}_g]_{t+\Delta t} + \ddot{\mathbf{v}}_{t+\Delta t}) + \mathbf{R}_t^g - \mathbf{F}_t - \mathbf{C}_t \dot{\mathbf{v}}_{t+\Delta t} \tag{5}$$

In this equation, $\mathbf{M}_t$ is the stack mass matrix, $(\mathbf{K}_e)_t$ is the stack elastic stiffness matrix and $(\mathbf{K}_g)_t$ is the stack geometric stiffness matrix, all defined in a fixed global co-ordinate system for known equilibrium configuration at time t, $\ddot{\mathbf{v}}_{t+\Delta t}$ and $\dot{\mathbf{v}}_{t+\Delta t}$ are the vectors of relative acceleration and velocity, respectively, at time $t + \Delta t$, $\mathbf{1}_x$ is the vector of ones and zeros identifying the degrees of freedom in the direction of ground acceleration $[\ddot{v}_g]_{t+\Delta t}$, $\mathbf{R}_t^g$ is the equivalent nodal load vector due to gravity at time t, $\mathbf{F}_t$ is the internal resisting force vector at time t and $\mathbf{C}_t$ is the stack damping matrix. In this formulation, an instantaneous Rayleigh damping matrix is used to give specified damping in first two modes throughout the time history analysis, i.e.

$$\mathbf{C}_t = a_t \mathbf{M}_t + b_t (\mathbf{K}_e)_t \tag{6}$$

The coefficients a_t and b_t are computed from tangent frequencies in first two modes. It may be noted that the mass matrices of the elements in their local co-ordinate axes remain constant but the transformation matrices from local-to-global co-ordinates change due to change in geometry of the stack. Therefore, the global mass matrix changes with time.

Solution procedure

The linearized equation of motion at time $t + \Delta t$ [Equation (5)] is solved for incremental displacements, velocities and accelerations by direct time integration using Newmark's average acceleration scheme with $\beta = 0{\cdot}25$ and $\gamma = 0{\cdot}5$. However, the values obtained for displacements, velocities and accelerations at time $t + \Delta t$ by adding these increments to initial values of displacements, velocities and accelerations, respectively, at time t, may not satisfy the exact equations of equilibrium at time $t + \Delta t$. Therefore, iterations are performed using the Newton–Raphson scheme within each time step so that equilibrium is satisfied at time $t + \Delta t$. Mass and damping matrices at the beginning of a time step are kept constant for all iterations within that time step. After each iteration the solution is checked for convergence with respect to prescribed tolerances on the unbalanced forces, the incremental displacements and the incremental energy.

To ensure convergence to right solution, repeated analyses were performed for typical stacks with reducing time steps of integration. It was observed that a very small time step, i.e. 0·0005 sec, needs to be used in numerical integration scheme to achieve convergence of all response quantities for the stacks. However, using such a small time step throughout the ground excitation record requires prohibitive computational efforts. Therefore, an adaptive time-step reduction procedure has been used in which the time step is halved when strain increment in any strip, or in a reinforcing bar, at any of the Gauss points exceeds 25 per cent of the yield strain of reinforcing steel, or when the incremental moment at any Gauss point exceeds 5 per cent of the moment capacity at that section. The limit on the strain increment ensures a smooth change in equilibrium configuration. The limit on the incremental moment restricts rapid change in forces due to closing of cracks or unloading in any step. Apart from these two limits, the time step is halved if convergence is not achieved after four iterations for equilibrium in a time step. The response results obtained using a normal time step of 0·02 sec with adaptive time-step reduction have been found to be in excellent match with those obtained with a constant time step of 0·0005 sec. The computational effort required in the former approach was substantially reduced.

Response quantities

Once the nodal displacement increments are known, strain increment at any point within the element is obtained from the strain displacement relations [Equation (2)]. The incremental strains are added to the

strains at time t to obtain the current state of strain. From these strains, stresses are calculated from appropriate stress–strain curves. Bending moment at each Gauss point is computed by taking moment of the forces in the concrete layers and reinforcing steel bars about the centroidal axis of the section. Equivalent moments at the two ends of an element are used to compute the constant shear force in that element. Axial force at Gauss point is computed by adding the forces in concrete layers and reinforcing bars. Axial force in an element is taken as the average of computed axial forces at the Gauss points.

The total seismic input energy, E_i, is computed from the absolute energy formulation using the following equation:[9]

$$E_i = \int (\ddot{\mathbf{v}}_t^{tot})^T \mathbf{M}_t \, d\mathbf{v}_g \tag{7}$$

in which $\ddot{\mathbf{v}}_t^{tot}$ is the total acceleration vector at time t, and $\mathbf{v}_g$ is a vector defined by $\mathbf{1}_x v_g$, where v_g is the ground displacement at time t and $\mathbf{1}_x$ is the vector of ones and zeros identifying the degrees of freedom in the direction of ground acceleration. The correctness of the solution is ensured by satisfying the energy balance equation. This is achieved by independently re-computing the total seismic input energy as a sum of total kinetic energy, total deformation energy, and damping energy. The total deformation energy includes both recoverable elastic energy and non-recoverable hysteretic energy.

EXAMPLE STACKS AND GROUND MOTIONS

The reinforced concrete stacks considered are of height 75, 150, and 300 m, each having the ratio of height to outer diameter at base equal to 15. A typical stack is shown in Figure 1. All stacks are linearly tapered with the outer diameter at top equal to half the outer diameter at the base. The thickness of shell is so chosen as to give the ratio of inner to outer diameter at base and at top equal to 0·95 but with a minimum shell thickness of 150 mm. The mass density of the stack shell is assumed to be 2500 kg/m^3 for the 75 m high stack and 3000 kg/m^3 for the 150 and 300 m high stacks in order to give axial stress in concrete at the base due to self-weight equal to $0{\cdot}1\sigma_{cy}$, $0{\cdot}2\sigma_{cy}$ and $0{\cdot}4\sigma_{cy}$ for the 75, 150 and 300 m high stacks, respectively. In this, σ_{cy} is the maximum permissible compressive stress in concrete. Two values of longitudinal reinforcement percentages, 0·25 and 0·5 per cent of the area of concrete, are considered. Details of the six example stacks are summarized in Table I.

Material properties of concrete and reinforcing steel are same for all six stacks. In presenting numerical results, the maximum permissible compressive stress, σ_{cy}, of concrete is taken 13·33 MPa. This value corresponds to concrete with characteristic cube strength of 20 MPa without any partial safety factor for material. This value represents the lowest grade of concrete permitted for the construction of stack-like structures in developing countries. The parameters defining the stress–strain curve of reinforcing steel are taken as: $\sigma_{sy} = 380$ MPa, $E_s = 2 \times 10^5$ MPa, $E_{sh} = E_s/200$. The ultimate compressive strain, ε_{cu}, in concrete is taken as 0.005 and the ultimate tensile strain in any of the reinforcing steel bars, ε_{su}, is assumed to be 0·1. The values of ε_{cu} and ε_{su} taken in presenting numerical results are lower than what are usually obtained experimentally. These limits on maximum compressive strain in concrete and maximum tensile strain in reinforcing steel implicitly define appropriate limit on the maximum curvature in annular reinforced concrete sections.

For non-linear analysis, each stack is idealized by 20 equal beam elements and three Gauss points are taken in each element. At each Gauss point the section is divided into 72 strips. Two hundred equally spaced reinforcing steel bars are considered in each of the two longitudinal reinforcing steel layers to give the required percentage of reinforcement. The normal time step of integration is taken 0·02 sec for all stacks with adaptive reduction of time step as described earlier. Three per cent damping in first two modes is considered in the instantaneous Rayleigh damping formulation of the damping matrix.

The stacks are analysed for a single horizontal component of the free-field ground acceleration. Five simulated acceleration time histories are generated[10] that are similar in frequency content but different in

Table I. Details of example reinforced concrete stacks and numerical results

Stack no.	Height (m)	Outer diameter at base D^*_{ob} (m)	Longitudinal reinforcement percentage	Axial stress in concrete due to self-weight	Average PGA of EDSE† (g)	Average PGA of MSE† (g)	Displacement ductility capacity factors for stacks	$\sqrt{ER}$‡	Maximum curvature ductility factor demand for cross-sections	Range of Y_h/H for plastic hinge	$\frac{V_{bnl(mce)}}{V_{bel(dbe)}}$
1	300	20	0·25	$0{\cdot}4\,\sigma_{cy}$	0·24	0·70	2·89	2·92	4·50	0·65–0·85	2·10
2	150	10	0·25	$0{\cdot}2\,\sigma_{cy}$	0·18	0·90	5·01	5·35	9·74	0·60–0·80	2·37
3	75	5	0·25	$0{\cdot}1\,\sigma_{cy}$	0·15	1·08	7·02	7·12	13·18	0·55–0·75	2·45
4	300	20	0·50	$0{\cdot}4\,\sigma_{cy}$	0·30	0·73	2·40	2·50	4·07	0·60–0·85	1·80
5	150	10	0·50	$0{\cdot}2\,\sigma_{cy}$	0·25	1·02	4·07	4·17	6·35	0·60–0·75	1·92
6	75	5	0·50	$0{\cdot}1\,\sigma_{cy}$	0·21	1·10	5·10	5·70	8·41	0·55–0·75	2·00

* The ratio of inner to outer diameter is 0·95 at the base of all stacks
† EDSE, elastic design strength earthquakes; MSE, maximum sustainable earthquakes
‡ ER is the average ratio of total seismic input energy for maximum sustainable earthquake to that for elastic design strength earthquake

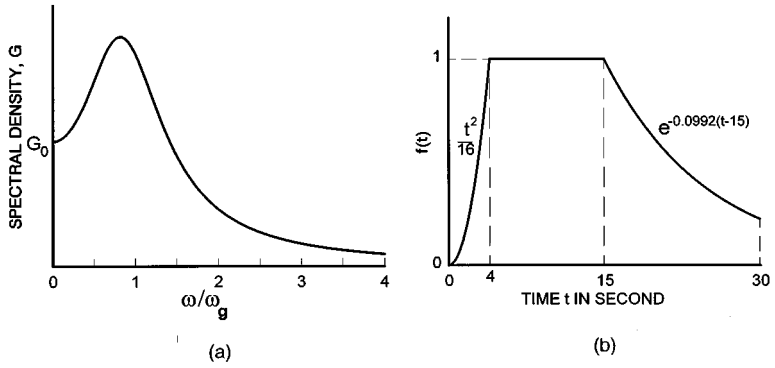

Figure 4. For simulated ground motions (a) spectral density function and; (b) intensity–time function

details for use in this study. The spectral density function defining the frequency contents of simulated motions is taken in the following form:[11,12]

$$G(\omega) = G_0 \frac{1 + 4\xi_g^2(\omega/\omega_g)^2}{[1 - (\omega/\omega_g)^2]^2 + 4\xi_g^2(\omega/\omega_g)^2} \tag{8}$$

with ground frequency $\omega_g = 4\pi$ and ground damping $\xi_g = 0.6$, suggested for firm ground sites (Figure 4). The scale of the power spectral density function, G_0, is selected such that it gives peak ground accelerations for the five simulated ground motions approximately equal to 1.0 g. The intensity function applied to simulated time histories to impart the transient nature of an actual earthquake is also shown in Figure 4. A parabolic base-line correction is performed on the generated ground motions. The resulting ground motions are presented in Figure 5. In predicting the desired results, the average of the responses for the five ground motions has been used because the variability in response obtained by time integration using simulated motions reflects only the inherent uncertainty due to random phasing, and not due to ground motion parameters such as duration and dominant ground frequency.[10]

SEISMIC CAPACITY

Inelastic seismic resistance

The definition of collapse for reinforced concrete stacks as a whole is quite subjective and depends on engineering judgment. One commonly used criteria of maximum inter-storey drift, as in multi-storey buildings, is not applicable for stacks because limitations on inter-storey drift is primarily to avoid damage to non-structural elements. The lateral displacement limit therefore may not be appropriate to define collapse of a stack. Failure in shear is not considered to define collapse because stacks usually fail in flexure. Moreover, part of the shear in stacks is resisted by concrete and the rest by circumferential reinforcement that can be increased to account for the increased shear force with little difficulty. Therefore, material failure criteria is used to define collapse of stacks in the present study. A stack is assumed to have reached its limit state of collapse if compressive strain in concrete at any of the Gauss points exceeds the maximum permissible compressive strain for concrete, which is taken as 0.005, or tensile strain in any of the reinforcing steel bars at a Gauss points exceeds the maximum permissible tensile strain for steel which is taken as 0·1.

For a stack, repeated non-linear earthquake analyses are performed for a simulated ground motion with gradually increasing intensity by adjusting the peak ground acceleration (PGA) in steps of 0·05g . The value of PGA for which the stack reaches its limit state of collapse is selected as ultimate value of PGA for that particular acceleration time history. This is repeated for all five simulated ground motions. Thus, a set of

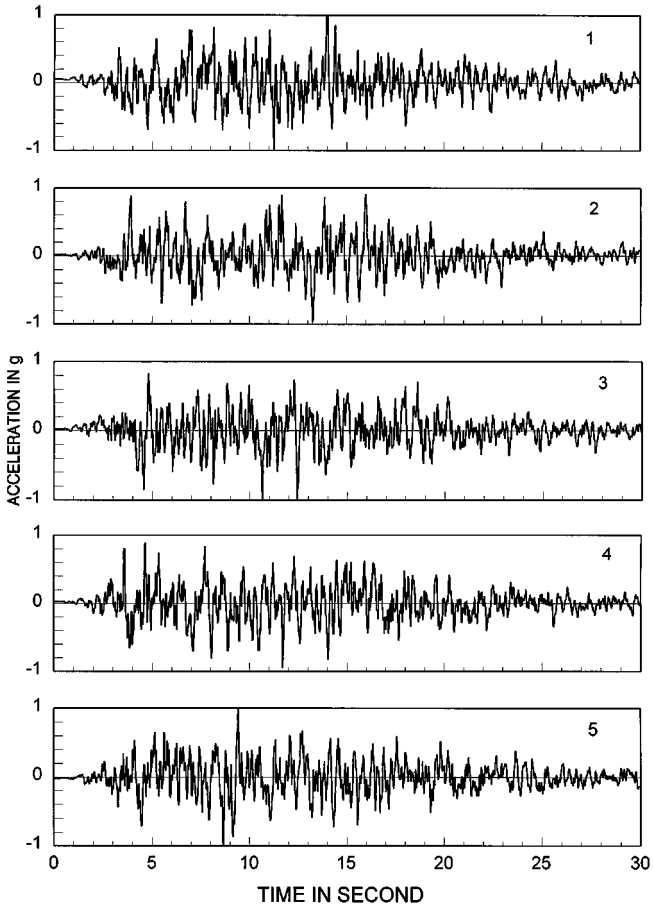

Figure 5. Acceleration time histories of simulated ground motions

acceleration time histories is obtained that the stack can sustain without collapse. The average elastic response spectrum for these five ground acceleration time histories with ultimate values of PGA is computed. This spectrum represents the intense ground motion that the stack can sustain if permitted to go in the inelastic range. This spectrum has been defined as the *maximum sustainable earthquake spectrum* for the stack, and has been taken as the representative of inelastic seismic resistance of the stack.

Elastic seismic resistance

In the elastic design procedure, moment at a single section exceeding the moment capacity is considered as failure of the stack. Therefore, to evaluate elastic seismic resistance, the moment capacities of cross-sections, with appropriate axial force due to self-weight applied at the cross-sections, are computed using the actual stress–strain relationships of concrete and reinforcing steel. The variation in the axial force level at a section due to horizontal ground excitation is usually small and, therefore, has been neglected in computing the moment capacities.

For a simulated ground motion with fixed value of PGA, each stack is analysed assuming its linear elastic behaviour. The PGA value of acceleration time history is linearly adjusted such that the moment capacity is reached at a single Gauss point and moments at all other Gauss points are less than their corresponding

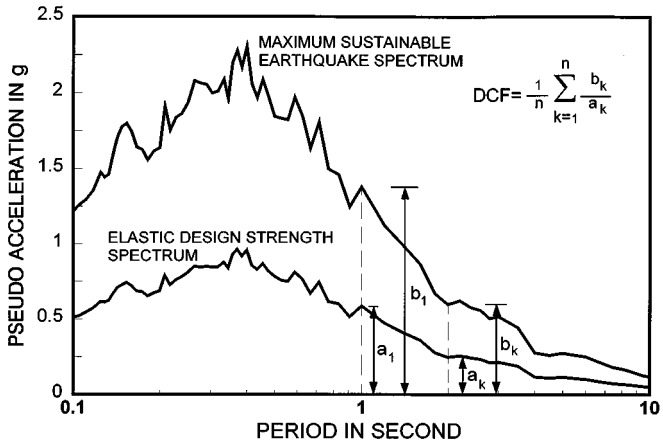

Figure 6. Computation of displacement ductility capacity factor (DCF) from maximum sustainable earthquake spectrum and elastic design strength earthquake spectrum

capacities. This is repeated for all five simulated ground motions. Thus, a set of acceleration time histories is obtained that the stack can sustain without inelastic deformations. The average elastic response spectrum for these five ground acceleration time histories with corresponding values of PGA is computed. This spectrum represents the intense ground motion that the stack can sustain based on its elastic strength. This spectrum has been defined as *elastic design strength spectrum* for the stack, and has been taken as the representative of elastic seismic resistance of stack.

Ductility capacity factor

For an elastoplastic system with specified displacement ductility capacity factor, μ, the design basis earthquake (DBE) spectrum with a specified exceedance probability can be derived by constructing constant-ductility response spectrum for many plausible ground motions for the site. Alternatively, a constant-ductility DBE spectrum can be constructed by multiplying the elastic response spectrum for the maximum credible earthquake (MCE) anticipated at that site by $1/\sqrt{2\mu - 1}$ in the acceleration-sensitive region (short period region), and by $1/\mu$ in the velocity and displacement sensitive regions (medium and long period regions).[13] The design forces in an elastoplastic system are then computed using elastic analysis from the constant-ductility design basis earthquake (DBE) spectrum, and the system is designed to have the specified ductility.

For a typical stack (Case 4 of Table I), the computed maximum sustainable earthquake (MSE) spectrum and the elastic design strength earthquake (EDSE) spectrum both with 3 per cent damping are presented in Figure 6. If for this stack, the MSE spectrum is taken as the maximum credible earthquake (MCE) spectrum, it may be stated that the stack is designed for MCE if permitted to undergo inelastic deformations (stack does not reach its limit state of collapse). Moreover, by definition, the EDSE spectrum for that stack is equivalent to its design basis earthquake spectrum (moment capacity does not exceed at any cross-section). Therefore, following the procedure mentioned above for deriving DBE spectrum from MCE spectrum, the overall displacement ductility capacity factor, μ, for long period structures like reinforced concrete stacks can be defined as an average of ratios of the ordinates of maximum sustainable earthquake spectrum to those of elastic design strength spectrum (Figure 6).

NUMERICAL RESULTS

The displacement ductility capacity factors (DCFs) have been estimated from the above-mentioned procedure for all six example stacks. Twenty-five equally spaced period values on logarithmic scale between 1 and

10 sec have been used in the averaging process to compute DCFs. The numerical values of DCFs obtained for example stacks are presented in Table I. The available ductility capacity reduces with increase in axial stress due to self-weight because maximum compressive strain in concrete is reached without significant yielding of reinforcing steel. Stacks with lesser longitudinal reinforcement percentage have higher available ductility capacity, since significant yielding of reinforcing steel occurs before maximum compressive strain in concrete is reached. For similar stacks, design basis earthquake spectrum in the velocity and displacement sensitive regions can be constructed by dividing the elastic response spectrum for the maximum credible earthquake by the displacement ductility capacity factors presented in Table I.

For each example stack, comparison is presented in Table I of DCF with the square root of the ratio of total input energies for maximum sustainable earthquake and the elastic design strength earthquake. The square root of the ratio of the total input energies is close to ductility factor for all stacks. These ductility factors, as computed in the present study, are closely related to the ratio of the PGA of the two sets of ground motions. This suggests the relation that scaling of ground motion by a factor α will lead to a corresponding scaling factor of α^2 for the total input energy for reinforced concrete stack-like structures. This has been established earlier for single-degree-of-freedom systems[14] and ductile moment-resisting frames[15] in the inelastic range.

It is apparent that the proportioning and detailing of a stack for the bending moments computed using the DBE spectrum (derived from MCE spectrum utilizing the ductility factors presented in Table I) will ensure that the stacks do not reach the limit state of collapse in the event of MCE. However, to utilize the full inelastic seismic resistance, it is necessary that stack cross-sections where plastic hinge may form have sufficient curvature ductility factor capacity. For each simulated ground motion, the maximum curvature of the cross-section at plastic hinge is obtained from time-history analysis. Knowing the yield curvature of the cross-section, the maximum curvature ductility factor demand for that cross-section is computed for each ground motion. The average value for five ground motions of the maximum curvature ductility factor demand for cross-sections at plastic hinges is taken as the curvature ductility factor demand for that stack. These values are presented in Table I for example stacks. The normalized distance of plastic hinge formation from the base, Y_h/H where H is the height of the stack, depends on the ground motion. For example stacks, the range Y_h/H of in which plastic hinge formation takes place is also presented in Table I. Designer must detail stacks to have curvature ductility factor capacity of cross-sections where plastic hinge may form higher than the values presented in Table I to utilize the full inelastic seismic resistance.

For the six stacks analysed, the average values of maximum shear forces at base obtained from the non-linear analysis for ground motions representing MSE, $V_{\mathrm{bnl(mce)}}$, have been observed to be significantly higher than the respective values obtained from the linear elastic analysis for ground motions representing DBE, $V_{\mathrm{bel(dbe)}}$. This implies that if a stack is designed for DBE deduced from MCE utilizing the ductility factors presented in Table I with the anticipation of ductile behaviour in flexure, the design shear forces for the stack obtained from DBE using elastic analysis must be enhanced. This aspect of the earthquake resistant design of stack-like structures is not included in any of the design codes even though ductile behaviour is implicit in the provisions for design forces in some codes.[1] Similar requirements of increased shear forces for reinforced concrete walls have been suggested by Aktan and Bertero.[16]

This aspect can be incorporated in seismic design of stacks by computing the base shear from DBE spectrum, and enhancing it by multiplying with the ratio, $V_{\mathrm{bnl(mce)}}/V_{\mathrm{bel(dbe)}}$. The average values of this ratio, $V_{\mathrm{bnl(mce)}}/V_{\mathrm{bel(dbe)}}$, for example stacks are presented in Table I. In simplified design procedures, this ratio can be introduced as *shear enhancement factor* . In most cases, however, shear strength provided by concrete and minimum circumferential reinforcement has been found to be sufficient to resist enhanced shear force.

CONCLUSIONS

A method is presented to estimate the inelastic seismic resistance of reinforced concrete stacks by non-linear dynamic analyses. It has been demonstrated that if inelastic deformations are permitted, the

actual seismic resistance of stack is much higher compared to what has been assumed in design. A procedure is also presented to quantify the difference between inelastic seismic resistance and elastic seismic resistance in terms of displacement ductility capacity factors. These DCFs can be used in deriving the design basis earthquake spectrum from the maximum credible earthquake spectrum for similar stacks. The corresponding values of curvature ductility factor demand for the cross-section of stacks at possible locations for plastic hinge formation are also presented. However, whenever the ductile behavior of stacks is considered in design, the values of corresponding design shear force obtained from DBE spectrum needs to be enhanced.

The behaviour of stacks in the inelastic range depends on ground motion, and therefore it may be necessary that the values of ductility capacity factors and shear enhancement factors suggested in this study be verified for other ground acceleration records, and re-established by experimentation with shaking table tests before incorporating them as recommendations in design codes.

APPENDIX

Notations

a_t	time-dependent coefficient of mass matrix in Rayleigh damping matrix
b_t	time-dependent coefficient of stiffness matrix in Rayleigh damping matrix
$\mathbf{C}_t$	damping matrix for stack at time t
E_c	modulus of elasticity of concrete
E_i	seismic input energy
E_s	modulus of elasticity of reinforcing steel
E_{sh}	straining hardening modulus of reinforcing steel
F_c	modulus of elasticity factor for concrete
F_t	internal resisting force vector at time t
H	height of the stack
$(\mathbf{K}_e)_t$	elastic stiffness matrix for stack at time t
$(\mathbf{K}_g)_t$	geometric stiffness matrix for stack at time t
$\mathbf{M}_t$	mass matrix for stack at time t
$\mathbf{R}^g$	equivalent load vector due to gravity
Δt	incremental time step
u	displacement along the local x-axis
u_0	displacement of the reference axis along the local x-axis
v	displacement along the local y-axis
v_0	displacement of the reference axis along the local y-axis
v_g	ground displacement
$\ddot{v}_g$	ground acceleration
$V_{bel(dbe)}$	base shear for design basis earthquake
$V_{bnl(mce)}$	base shear for maximum credible earthquake
$\dot{\mathbf{v}}$	global velocity vector
$\ddot{\mathbf{v}}$	global acceleration vector
Y_h	distance of plastic hinge formation from the base
β	parameter in direct time integration
ε_c	strain in concrete
ε_{cy}	strain in concrete at maximum compressive stress
ε_{su}	ultimate strain of reinforcing steel
$\Delta\varepsilon$	incremental strain
γ	parameter in direct time integration

μ displacement ductility factor of elasto-plastic system
σ_c stress in concrete
σ_{cy} maximum compressive stress in concrete
σ_{sy} yield stress of reinforcing steel

REFERENCES

1. A. K. Chopra and C.-Y. Liaw, 'Earthquake resistant design of intake-outlet towers', *J. struct. div. ASCE* **101**, 1349–1366 (1975).
2. N. M. Newmark and E. Rosenblueth, *Fundamentals of Earthquake Engineering*, Prentice-Hall, Englewood Cliffs, NJ, 1971.
3. ACI 307-79, Specifications for Design and Construction of R.C. Chimneys, American Concrete Institute, Detroit, 1979.
4. D. Whittaker, R. Park and A. J. Carr, 'Experimental tests on hollow circular concrete columns for use in offshore concrete platforms', *Proc. Pacific conf. on earthquake engineering*, *Wairakei*, *Vol.* 1, 1987, pp. 213–224.
5. E. C. Chan, 'Nonlinear geometric, material and time dependent analysis of reinforced concrete shells with edge beams', *Report No. UCB/SESM-82/08*, Division of Structural Engineering and Structural Mechanics, University of California, Berkeley, CA, 1982.
6. K. J. Bathe and S. Bolourchi, 'Large displacement analysis of three-dimensional beam structures', *Int. j. numer. methods eng.* **14**, 961–986 (1979).
7. R. Park and T. Paulay, *Reinforced Concrete Structures*, J Wiley, New York, 1975.
8. K. J. Bathe, *Finite Element Procedures in Engineering Analysis*, Prentice-Hall, Englewood Cliffs, NJ, 1982.
9. C. M. Uang and V. V. Bertero, 'Evaluation of seismic energy in structures', *Earthquake eng. struct. dyn* . **19**, 77–90 (1990).
10. D. A. Gasparini and E. H. Vanmarcke, 'Simulated earthquake motions compatible with prescribed response spectra', *Department of Civil Eng. Research Report*, *R76-4(527)*, MIT, Cambridge, MA, 1976.
11. K. Kanai, 'An empirical formula for the spectrum of strong earthquake motions', *Bull. earthquake res. inst.* **39**, 85–95 (1961).
12. H. Tajimi, 'A statistical method of determining the maximum response of a building structure during an earthquake', *Proc. 2nd WCEE*, Tokyo, Vol. **2**, 1960, pp. 781–797.
13. A. K. Chopra, *Dynamics of Structures*, *Theory and Applications to Earthquake Engineering*, Prentice-Hall, Englewood Cliffs, NJ, 1995.
14. P. C. Jennings, 'Earthquake response of a yielding structure', *J. eng. mech. div. ASCE* **91**, 41–68 (1965).
15. W. K. Tso, T. J. Zhu and A. C. Heidebrecht, 'Seismic energy demands on reinforced concrete moment resisting frames', *Earthquake eng. struct. dyn.* **22**, 533–545 (1993).
16. A. E. Aktan and V. B. Bertero, 'RC structural walls: seismic design for shear', *J. struct. eng. ASCE* **111**, 1775–1791 (1985).

